Biomaterials 34 (2013) 275–282

Contents lists available at SciVerse ScienceDirect

Biomaterials

journal homepage: www.elsevier.com/locate/biomaterials

Sodium caprate as an enhancer of macromolecule permeation across tricellular tight junctions of intestinal cells

Susanne M. Krug [a], Maren Amasheh [b], Isabel Dittmann [a], Ilya Christoffel [a], Michael Fromm [a], Salah Amasheh [a,*]

[a] Institute of Clinical Physiology, Charité, Campus Benjamin Franklin, Freie Universität and Humboldt-Universität, 12200 Berlin, Germany
[b] Dept. of Gastroenterology, Div. of Nutritional Medicine, Charité, Campus Benjamin Franklin, Freie Universität and Humboldt-Universität, 12200 Berlin, Germany

ARTICLE INFO

Article history:
Received 27 July 2012
Accepted 21 September 2012
Available online 12 October 2012

Keywords:
Absorption
Electrophysiology
Epithelial cell
Drug delivery

ABSTRACT

Sodium caprate is a promising candidate for inducing drug absorption enhancement. The mechanism of that uptake-enhancing effect is not fully understood so far. We investigated how caprate acts in an established human intestinal cell line, HT-29/B6, on the transient opening of transcellular (across the cell membranes) and paracellular (across the tight junction) pathways. Sodium caprate (10 mM) caused a rapid and reversible decrease of transepithelial resistance which is based, as measured by two-path impedance spectroscopy, exclusively on resistance changes of the paracellular pathway. Measurements of paracellular marker fluxes revealed an increased permeability for fluorescein (330 Da) and FITC-dextran (4 and 10 kDa), indicating an opening of the paracellular barrier. Confocal microscopy revealed a marked reduction of tricellulin in tricellular tight junctions and of claudin-5 in bicellular tight junctions. This was not due to altered protein expression, as occludin, claudins or tricellulin were not significantly changed in Western blots. Visualization of the translocation site of the cell membrane-impermeable marker molecule sulpho-NHS-SS-biotin (607 Da) indicated the tricellular tight junction to be the predominant pathway. We suggest that caprate's known enhancing effect on intestinal drug uptake is based on increased permeability in tricellular cell contacts, mediated by reversible removal of tricellulin from the tricellular tight junction.

1. Introduction

A number of therapeutic substances are poorly absorbed and have inherently low oral bioavailability [1]. Absorption enhancers are discussed in context with the development of drug targeting and drug delivery strategies, enabling effective uptake of a wide range of pharmacological substances [2]. Uptake via the epithelial passage may occur via transcellular or paracellular processes. A plethora of substances does not meet the requirements for selective substrate recognition of transcellular transporters. Hydrophilic compounds, such as peptide- and protein-based medications cannot permeate across cell membranes and therefore are hindered to achieve certain desired therapeutic responses compared to lipophilic drugs. An exception might be specific membrane transporters, as demonstrated by the intestinal oligopeptide transporter PepT1, which recognizes peptidomimetics such as the β-lactam antibiotic ampicillin and 5-aminolevulinic acid as substrates [3–5]. Additionally, two sites of selective translocation are involved in transcellular permeation, namely the apical and the basolateral side of epithelia. A promising approach and more versatile strategy is to enhance the absorption of hydrophilic macromolecular drugs by co-administration of absorption-enhancing agents that reversibly open the paracellular barrier [6].

Several sodium salts of medium chain fatty acids are able to enhance the paracellular permeability of hydrophilic compounds. However, sodium caprate, the sodium salt of the aliphatic saturated 10-carbon medium chain fatty acid capric acid, is the only absorption-enhancing agent clinically employed as a component of a rectal ampicillin suppository [7]. It is also discussed in approaches focusing on the development of gene therapy of cystic fibrosis [8], and oral availability of insulin [9,10]. Capric acid is present in human milk, with a concentration of 0.2 mM [11], and in plant oils

* Corresponding author. Institute of Clinical Physiology, Charité – Universitätsmedizin Berlin, Campus Benjamin Franklin, 12200 Berlin, Germany. Tel.: +49 30 8445 2500; fax: +49 30 8445 4239.
E-mail address: salah.amasheh@charite.de (S. Amasheh).

0142-9612/$ – see front matter © 2012 Elsevier Ltd. All rights reserved.
http://dx.doi.org/10.1016/j.biomaterials.2012.09.051

like coconut and seed oils [12]. Because of its presence in food, sodium caprate is approved by the FDA as a direct food additive for human consumption [13].

The structural correlate of the paracellular barrier is the tight junction (TJ), a complex located in the apicolateral membrane of epithelial cells [14]. The TJ consists of proteins associated with the perijunctional actin cytoskeleton. Within this structure, a number of tetraspan TJ proteins has been reported, which interconnect the apicolateral membranes of neighboring cells, namely the family of claudins [15] and the TAMP (tight junction associated MARVEL protein [16]) family which consists of occludin [17], tricellulin [18], and MarvelD3 [19].

The family of claudins has a big variance in function for the paracellular barrier formed by the TJ, and expression profiles vary between different epithelial tissues, as demonstrated e.g. in detail for intestine [20], skin [21], mammary epithelium [22], pleura [23], as well as kidney and brain capillary endothelium [2,24]. Some claudins possess barrier tightening properties as it has been shown for e.g. claudin-1 [25], -3 [26], or -5 [27], while others form paracellular channels with ion selectivity, e.g. claudin-2 [28], -10b [29], and -15 [30] for small cations, and claudin-10a [29] and -17 [31] for small anions. Attempts have been made to modify claudin permeability e.g. by creation of claudin binders [32].

A major determinant for paracellular macromolecule permeability is provided by tricellulin [33]. Tricellulin is predominantly located within the tricellular TJ (tTJ; [18]). The tTJ is formed at the meeting point of three cells where three bicellular TJ (bTJ) strands converge. It extends far more basolaterally than the bTJ, forming a vertically orientated triple pair strand structure with a “central tube” [34–36]. This central tube is supposed to be a weak point of the paracellular barrier [37,38]. As a first hint that tricellulin is involved in that process came when in tricellulin knockdown studies a break-down of the whole TJ network occurred [18]. Using the opposite approach, in a subsequent study on low-tricellulin cells (MDCK II) we could show that tricellulin overexpression in tTJs tightens against macromolecule passage via the tTJ [33]. We wondered whether the opposite effect could be employed for reversibly enhancing the epithelial uptake of macromolecular drugs by removal of tricellulin.

For caprate it is known that it acts an absorption enhancer for macromolecules by modulating the paracellular pathway, however, in a yet not clearly defined way [39]. It has been shown on Caco-2-cells that caprate may act on the TJ by cytoskeletal contraction triggered by MLCK interaction [40–42].

In order to resolve the effect of caprate on the intestinal barrier in detail, we employed two-path impedance spectroscopy to determine the paracellular resistance, determined permeabilities for paracellular markers of different size, and performed expression and localization analysis of TJ proteins.

The goal of our study was to test the hypothesis that the mechanism of caprate’s effect on macromolecular passage is caused by alterations of the tricellular tight junctional pathway, and that tricellulin is the key player for that effect.

2. Material and methods

2.1. Cells and solutions

The human colon cell line HT-29/B6 exhibits a high transepithelial resistance, reacts on secretagogues with chloride and mucus secretion, and thus possesses basic properties of colonic epithelia [43]. It has been employed in numerous studies as a model epithelium and has been used recently for a detailed analysis of the effects of chitosan as an absorption enhancer [6].

Confluent monolayers of HT-29/B6 cells [43] were grown in 25 cm^2 culture flasks containing RPMI1640 with stable L-glutamine, 10% fetal calf serum, and 1% penicillin/streptomycin until confluence, as reported in more detail recently [6]. Cells were cultured at 37 °C in a humidified 5% CO_2 atmosphere. For electrophysiological measurements, HT-29/B6 cells were seeded on Millicell PCF filters (Millipore, Schwalbach, Germany), and experiments were performed after 7 days. The apical compartment was routinely filled with 500 µl culture medium, and the basolateral compartment contained 10 ml. For experiments, sodium caprate (194.25 Da, Sigma Aldrich, Taufkirchen, Germany) was added to bath Ringer solution containing 113.6 mM NaCl, 2.4 mM Na_2HPO_4, 0.6 mM NaH_2PO_4, 21 mM $NaHCO_3$, 5.4 mM KCl, 1.2 mM $CaCl_2$, 1.2 mM $MgCl_2$, and 10 mM D(+)-glucose.

2.2. Lactate dehydrogenase release assay

For analysis of caprate-mediated toxicity on HT-29/B6 cells, a lactate dehydrogenase (LDH) release assay was performed [44]. LDH, a cytosolic enzyme, is released into the culture medium when cells are injured. For this, the LDH level in 500 µl of the apical medium and in 500 µl of the cell lysate was determined under control conditions, and 2 h after application of sodium caprate, cell lysis was performed in PBS containing 2% Triton X-100.

2.3. Electrophysiology

2.3.1. Transepithelial resistance and paracellular marker flux measurements

Confluent cell monolayers were grown on permeable supports (Millipore, Schwalbach, Germany), and these inserts were mounted in custom-designed Ussing chambers [43]. Water-jacketed gas lifts were filled with 5 ml circulating fluid on each side, containing 113.6 mM NaCl, 2.4 mM Na_2HPO_4, 0.6 mM NaH_2PO_4, 21 mM $NaHCO_3$, 5.4 mM KCl, 1.2 mM $CaCl_2$, 1.2 mM $MgCl_2$, and 10 mM D(+)-glucose. The solution was constantly gassed with 95% O_2 and 5% CO_2. The temperature of the bath solution was kept at 37 °C. Transepithelial resistance (TER) was calculated from voltage changes (ΔV) induced by short current pulses (50 µA, 0.3 s). All experimental data were corrected for values of empty filter and the bath solution.

Paracellular marker flux analyses were performed in Ussing chambers under voltage-clamp conditions (0 mV). 0.4 mM dialyzed FITC-labeled dextran (FD4, FD10, FD20 with 4, 10, and 20 kDa, respectively) was added to the apical side, and basolateral samples were collected every 30 min and replaced by fresh perfusion solution. Three flux periods of 30 min were analyzed after application of sodium caprate compared to controls. Dextran fluxes were calculated from the amount of FITC-dextran in the basolateral compartment which was measured with a fluorometer at 520 nm (Tecan Infinite M200, Tecan, Switzerland).

2.3.2. Two-path impedance spectroscopy

Epithelial resistance (R^{epi}), transcellular resistance (R^{trans}) and paracellular resistance (R^{para}) of HT-29/B6 monolayers were measured by two-path impedance spectroscopy as described in detail recently [45]. Briefly, filters were mounted in Ussing-type impedance chambers and bathed with Ringer’s solution. Application of alternating current (35 µA/cm^2, frequency range 1.3 Hz–65 kHz) resulted in changes of epithelial voltage which was detected by phase-sensitive amplifiers (402 frequency response analyzer, Beran Instruments; 1286 electrochemical interface; Solartron Schlumberger). Complex impedance (Z_{real}, $Z_{imaginary}$) values were calculated and plotted in a Nyquist diagram, showing the capacitive components (the imaginary parts of the complex impedance value) against the ohmic components (the real part of the complex value). R^{epi} equals TER minus the contribution of non-epithelial barriers, which is provided in cell cultures by the filter membrane (R^{sub}). The values for R^{sub} and R^{epi} were used for further calculation. In order to discriminate R^{para} and R^{trans}, fluxes of a paracellular marker, fluorescein, were measured before and after Ca^{2+} removal using ethylene glycol tetraacetic acid (EGTA). EGTA caused TJs to partly open and to increase fluorescein flux which was inversely proportional to changes of R^{para}. The resulting impedance spectra and the fluxes before and after chelating extracellular Ca^{2+} were used for final determination of R^{trans} and R^{para} [45].

2.4. Detection of tight junction proteins

2.4.1. Immunohistochemistry

Immunofluorescent staining and analysis by confocal laser-scanning microscopy were performed as described in detail previously [6]. Confluent cell monolayers grown on permeable supports were incubated with sodium caprate, cells were rinsed with PBS, fixed with methanol, and permeabilized with PBS containing 0.5% Triton X-100. Immunofluorescent staining was performed with antibodies raised against occludin, tricellulin, and claudins. Concentrations of primary antibodies were 10 µg/ml. As secondary antibodies Alexa Fluor 488 goat anti-mouse, and Alexa Fluor 594 goat anti-rabbit were used at concentrations of 2 µg/ml. DAPI (4′,6-diamidino-2-phenylindole dihydrochloride) was used to stain cell nuclei, and FITC-phalloidin to stain F-actin. Fluorescence images were obtained with a confocal microscope (LSM 510 Meta, Carl Zeiss, Jena, Germany) using excitation wavelengths of 543, 488, and 405 nm, respectively.

For visualization of macromolecule passage across the tight junction, cells were apically labeled with sulfosuccinimidyl-2-(biotinamido)-ethyl-1,3′-dithiopropionate (sulfo-NHS-SS-biotin). Sulfo-NHS-SS-biotin (606.7 Da) is a cleavable, water-soluble, amino-reactive biotinylation reagent, which is cell membrane impermeable due to its sodium sulfonate group. After 2 min, cells were fixed and an

immunofluorescent staining of the apicolateral tight junction complexes was performed with mouse anti-ZO-1.

2.4.2. Western blot experiments

Immunoblots were performed as described previously [6]. Cells were either homogenized in total lysis buffer containing 10 mM Tris, 150 mM NaCl, 0.5% Triton X-100, and 0.1% sodium dodecyl sulfate (SDS), or buffer containing 20 mM Tris, 5 mM $MgCl_2$, 1 mM ethylenediaminetetraacetic acid (EDTA) and 0.3 mM EGTA for preparation of membrane fractions. Prior to lysis, protease inhibitors were added to lysis buffers, respectively (Complete, Boehringer, Mannheim, Germany). After preparation, protein contents were determined using bicinchoninic acid (BCA) protein assay reagent (Pierce, Rockford, IL, USA) and quantified with a plate reader (Tecan, Grodig, Austria). Samples were mixed with SDS buffer (Laemmli), loaded on a 12.5% SDS polyacrylamide gel and electrophoresed. Proteins were detected by immunoblotting employing primary antibodies raised against occludin, tricellulin, or claudin-1, -2, -3, -4, -5, and -8, and β-actin. Peroxidase-conjugated goat anti-rabbit IgG or goat anti-mouse IgG antibodies and the chemiluminescence detection system LumiLightPLUS Western blotting kit (Roche, Mannheim, Germany) were used to detect bound antibodies. Signals were visualized by luminescence imaging (Fusion FX7, Vilber Lourmat, France).

2.5. Chemicals

All chemicals, unless otherwise noted, were purchased from Sigma Aldrich. Antibodies raised against claudins and occludin were purchased from Invitrogen (Zymed Labs, San Francisco, CA). The antibodies against tricellulin (C-term) and against β-actin were purchased from Sigma–Aldrich. Secondary antibodies, Alexa Fluor 488 goat anti-mouse and Alexa Fluor 594 goat anti-rabbit were purchased from Molecular Probes (MoBiTec, Göttingen, Germany).

2.6. Statistical analysis

Data are expressed as means ± standard error of the mean. Statistical analysis was performed using Student's *t*-test and the Bonferroni–Holm correction for multiple comparisons. $p < 0.05$ was considered significant. Significance levels are denoted n.s. = not significantly different, $^{*} = p < 0.05$, $^{**} = p < 0.01$, $^{***} = p < 0.001$. The number of experiments is indicated by *n*.

3. Results

3.1. Measurement of transepithelial, transcellular, and paracellular resistance

Transepithelial resistance (TER) measurements after apical addition of 3, 10, and 30 mM sodium caprate lead to concentration- and time-dependent effects as shown in Fig. 1A. During the time course of the experiment, TER of controls remained constant (t_0: 680.3 ± 19.8 Ω cm^2 and t_{120}: 702.4 ± 32.2 Ω cm^2, $n = 12$, respectively). Caprate (10 mM) induced a rapid and consistent drop of TER to ~50% of initial values (t_0: 705.5 ± 31.5 Ω cm^2 to t_{30}: 373.4 ± 24.4 Ω cm^2, $^{***}p < 0.001$, $n = 12$). A threefold higher caprate concentration did not lead to significantly stronger effects on TER compared to 10 mM (t_0: 638.7 ± 47.6 Ω cm^2; t_{30}: 297.9 ± 34.5 Ω cm^2, $^{***}p < 0.001$, $n = 9$), whereas the effect of 3 mM was less pronounced after 30 min (616.9 ± 37.2 Ω cm^2), reached a maximum after 60 min (t_0: 543.4 ± 28.9 Ω cm^2, $^{**}p < 0.01$, $n = 9$), but returned to initial control values prior to wash out at t_{120} (n.s. from controls). As 10 mM sodium caprate showed maximum effects on TER this concentration was chosen for further experiments. Effects of 10 mM were reversible after wash out (632.3 ± 29.2 Ω cm^2, n.s., $n = 12$).

For discrimination between the transcellular and the paracellular pathway, two-path impedance spectroscopy was performed (Fig. 1B). In this set of experiments, the transepithelial resistance (R^{epi}) decreased from 863.4 ± 40.7 to 546.95 Ω cm^2 after addition of sodium caprate ($^{*}p < 0.001$, $n = 6$). The transcellular resistance (R^{trans}) did not change significantly (1151.8 ± 40.5 and 1090.4 ± 62.2 Ω cm^2, $n = 6$), whereas a marked decrease of the paracellular resistance (R^{para}) was observed (from 3699 ± 540.5 to 1119.5 ± 79.7 Ω cm^2, $^{***}p < 0.001$, $n = 6$), indicating a purely paracellular effect of caprate.

3.2. Measurement of cell viability

To exclude toxic effects, cell viability under control conditions and after 2 h exposure to 10 mM sodium caprate was tested by LDH release assay. This assay reveals the activity of the cytosolic enzyme LDH, which is elevated under toxic conditions as it is released into the medium when cells are injured. As depicted in Fig. 2, the assay revealed no significant change of LDH release during the time course of the experiment ($n = 4$).

3.3. Measurement of paracellular flux markers

To evaluate the size-selectivity of the paracellular pathway, the permeabilities for fluorescein, and 4, 10, and 20 kDa FITC-dextran (FD4, FD10, and FD20) were analyzed in unidirectional marker flux experiments (Fig. 3). Permeability for fluorescein was markedly increased in the caprate group (10 mM) compared to controls (from 2.08 ± 0.21·10^{-5} to 6.32 ± 0.92·10^{-5} cm/s) and the same was true for the two smaller FITC-dextrans (FD4 from 0.82 ± 0.08·10^{-5} to 1.71 ± 0.21·10^{-5} cm/s and FD10 from 0.40 ± 0.03·10^{-5} to 1.08 ± 0.15·10^{-5} cm/s). In contrast, permeability for FD20 was not

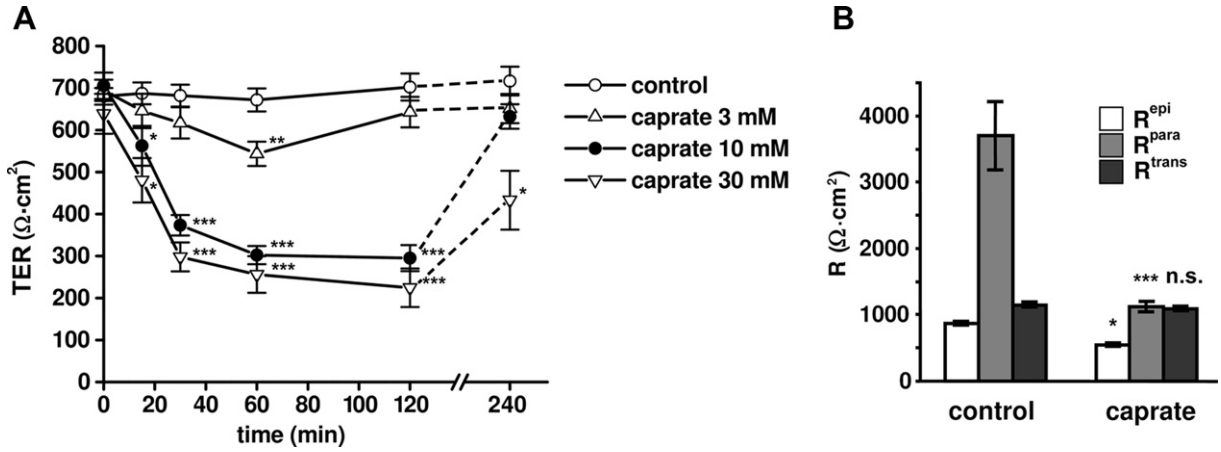

Fig. 1. A: Time and concentration response in HT-29/B6 cells. Incubation with 3, 10 and 30 mM sodium caprate resulted in a decrease of transepithelial resistance. Whereas effects of 3 mM returned to control values after 120 min, 10 and 30 mM had a strong and consistent effect for 120 min on TER ($^{*}p < 0.05$, $^{**}p < 0.01$, $^{***}p < 0.001$, $n = 9$–12, respectively). B: Two-path impedance spectroscopy. Sodium caprate decreased transepithelial resistance R^{epi} by an effect on the paracellular resistance R^{para}. In contrast, transcellular resistance (R^{trans}) was not changed indicating an exclusive effect on paracellular barrier properties ($^{*}p < 0.05$, $^{***}p < 0.001$, $n = 6$).

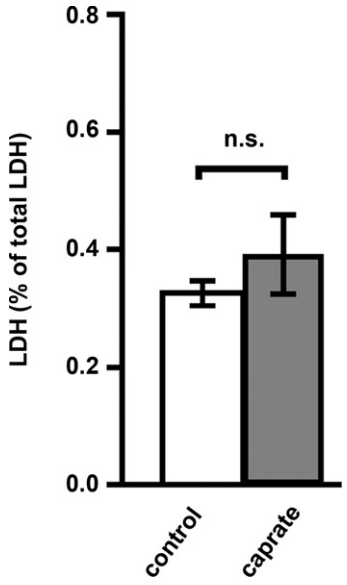

Fig. 2. Cell viability LDH assay. Cell viability was tested with the lactate dehydrogenase (LDH) release assay. As an indicator of cell disruption the LDH release from the cells was measured in apical medium and in whole cell lysates. The total LDH content of the cells was set as 100% and LDH released into the medium was calculated. After 2 h exposure to 10 mM caprate no significant change occurred (n.s., $n = 4$).

significantly changed (from $0.04 \pm 0.04 \cdot 10^{-5}$ to $0.06 \pm 0.03 \cdot 10^{-5}$ cm/s), indicating an opening of the paracellular pathway for macromolecules up to 10 kDa.

3.4. Analysis of the cytoskeleton

Effects of caprate (10 mM) on the cytoskeleton were analyzed employing confocal laser-scanning immunofluorescence microscopy for analysis of F-actin-stained cells, and inhibitors of actin–myosin interaction. Immunofluorescent stainings did not reveal changes in the localization and integrity of the perijunctional actomyosin ring, indicating no effect on cytoskeletal structures (Fig. 4A). Moreover, inhibitors of actin–myosin interaction as myosin light chain kinase blockers inhibitory peptide M18 (10^{-5} M, apical and basolateral, $n = 4$) and ML-7 (10^{-5} M, apical and basolateral, $n = 4$), Rho kinase inhibitor Y-27632 (10^{-5} M, apical and basolateral, $n = 4$), the Ca^{2+} chelator BAPTA-AM, ($2 \cdot 10^{-5}$, apical and basolateral, $n = 4$), and the phospholipase C inhibitor U73122 (10^{-5} M, apical and basolateral, $n = 4$) did not inhibit the effect of 10 mM caprate effect (Fig. 4B).

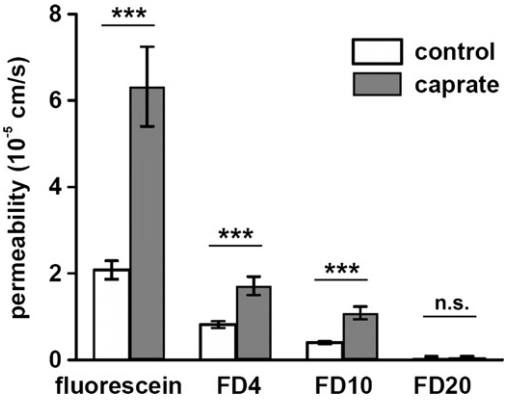

Fig. 3. Effect of caprate on the permeability for paracellular flux markers. Paracellular marker flux measurements employing fluorescein, 4, 10, and 20 kDa FITC-dextran revealed marked effects on the permeability of molecules to a size of 10 kDa, whereas the passage of 20 kDa dextran was not significantly changed (***$p < 0.001$, $n = 4$–7).

3.5. Analysis of tight junction proteins

For analysis of the effect of caprate on TJ proteins, Western blots were performed employing total protein lysates as well as membrane fractions of cell monolayers incubated with 10 mM sodium caprate (Fig. 5). No obvious changes of TJ proteins claudin-1, -2, -3, -4, -5, and -8, occludin, and tricellulin in both, total lysates and membrane fractions compared to respective β-actin signals of selfsame preparations were observed ($n = 6$, pooled filters).

Analysis of apicolateral TJ protein localization before and after incubation with sodium caprate by immunofluorescent stainings showed different effects. Tricellulin, counter-stained with occludin as TJ marker, revealed a selective decrease of tricellulin in tTJs after sodium caprate treatment, whereas occludin remained unchanged (Fig. 6A). After wash out of caprate, tricellulin was present in tTJs again (Fig. 6A). Moreover, a reversible decrease of claudin-5 signals in bTJs was observed after incubation with sodium caprate (Fig. 6B), whereas signals of two other sealing tight junction proteins, claudin-1 and -8, as well as a channel-forming protein, claudin-2, did not change (Fig. 6C).

3.6. Localization of permeation sites

To localize macromolecule permeation, monolayers were apically incubated with sulfo-NHS-SS-biotin (606.7 Da) after treatment with sodium caprate (Fig. 7), and then were counter-stained with anti-ZO-1 (green). Scanning of the lateral (*z*-)axis of the cells by means of confocal laser-scanning microscopy revealed specific localization of the red biotin signals within (a) and below (b) tricellular cell contacts, whereas below bicellular cell contacts of sodium caprate-treated cells (c) as well as in controls without sodium caprate, no biotin permeation was observed. This method detects translocated biotin trapped in the intercellular space, while apically remaining biotin was widely (but, due to technical imperfectness, not completely) washed out. Therefore, dependent on incubation and wash out time, some biotin can also remain apically. Such remnants do not signify translocation sites. In contrast, translocated biotin is located below the tight junction and is not affected by subsequent wash out, indicating that it indeed has translocated. In our study, such sites were limited to tricellular, but not bicellular, cell contacts.

4. Discussion

4.1. Analysis of caprate effects in HT-29/B6 epithelial cells

In our study, effects of caprate in HT-29/B6 epithelial cells were analyzed in detail. HT-29/B6 cells represent a valuable model for barrier analyses of intestinal colonic epithelia [43], with advantages such as high reproducibility in accordance with parallel studies in rodent and human intestinal tissues, and especially an endogenous expression of major barrier-forming tetraspan TJ proteins such as tricellulin [33], occludin, or claudins [27,46,47].

Sodium caprate is a natural compound with wide distribution as it is also present in food sources like milk, and a variety of plant oils. Although concentrations differ and remain markedly lower in food, even a high concentration of 10 mM does not have a toxic effect on HT-29/B6 cells as shown in our study. Moreover, a concentration of 3 mM also had an effect, but even, prior to wash out, spontaneously returned to control values where Ringer's solution only was added, which further supports physiological compatibility. In accordance with the non-toxic properties of sodium caprate shown in our

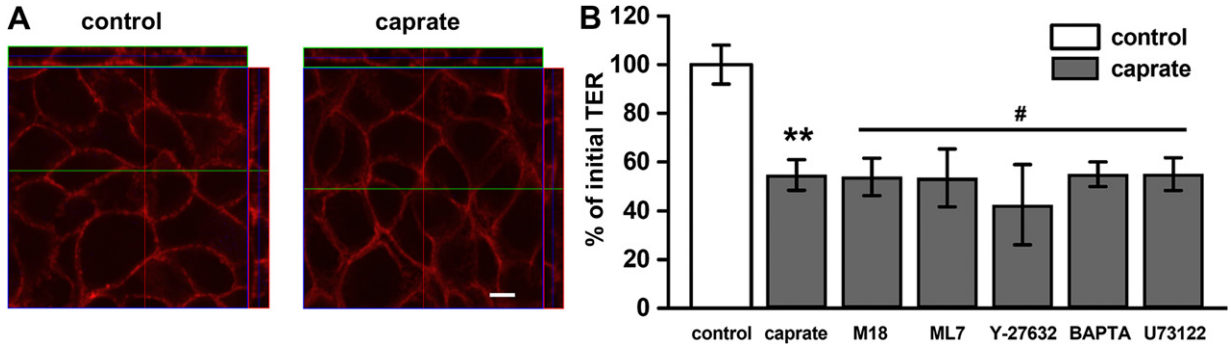

Fig. 4. Analyses of F-actin and inhibitors of actin-myosin interactions. (A) Immunostaining revealed no change in F-actin localization, as strong signals were detected in both, controls and caprate-induced cells within the perijunctional actomyosin ring. (B) Blockers of the actin–myosin interaction inhibitory peptide M18, ML-7, Rho kinase blocker Y-27632, BAPTA-AM, and phospholipase C blocker U73122 did not reveal an effect on sodium caprate-mediated decrease of transepithelial resistance ($^*p < 0.05$, #n.s. from caprate effect; $n = 4–7$).

study, the compound is marketed as a food additive and is regarded harmless, demonstrated by approval by the FDA [13]. An important application of sodium caprate is the clinically use as an enhancer for intestinal absorption [7]. Because of its safety profile it can be regarded superior to other agents of frequent consumption or use, as e.g. aspirin or alcohol [48,49]. The rapid and selective opening of the paracellular barrier makes it a promising candidate to promote intestinal availability of macromolecular drugs, which includes a wide variety of normally poorly absorbed molecules, and the possibility to reduce active concentrations to minimize potential adverse side effects. Moreover, spontaneous reversibility also reduces probability of adverse effects such as increased translocation of noxious agents through the intestinal wall which may trigger immunological responses.

4.2. Specific effects of caprate on the paracellular pathway

Measurement of two-path impedance spectroscopy revealed a pure paracellular effect of caprate. This is at variance to the effects of chitosan, a chitin derivative also used as an absorption enhancer [6], in which chitosan mediated decrease in TER of HT-29/B6 cells by both, a decrease of R^{para} as well as R^{trans}. In our experiment focusing on sodium caprate however, no effect on the R^{trans} could be observed. We conclude that this effect is mediated by removal of a sealing tight junction protein, claudin-5, from the tight junction.

However, electrical resistances (both, TER as well as the ohmic part of impedance) are reciprocal measures of the permeability for small inorganic ions (mainly Na, K, and Cl), so that this result might indicate, but does not fully explain the mechanism for enhanced uptake of larger molecules, as most drugs are.

Paracellular permeability after sodium caprate incubation has been reported for ampicillin [7], and larger molecules, such as insulin [9]. Whereas ampicillin derivatives have a molecular weight of 349 Da, insulin is considerably larger with a MW of 5.8 kDa. Therefore, paracellular FITC-labeled dextran marker fluxes of 4, 10, and 20 kDa were employed in our study to analyze size-selectivity of the paracellular pathway of HT-29/B6 cell monolayers treated with sodium caprate, demonstrating a permeability for molecules up to 10 kDa, which would include an increased permeability for the peptide hormone insulin, in accordance with observations *in situ* [9].

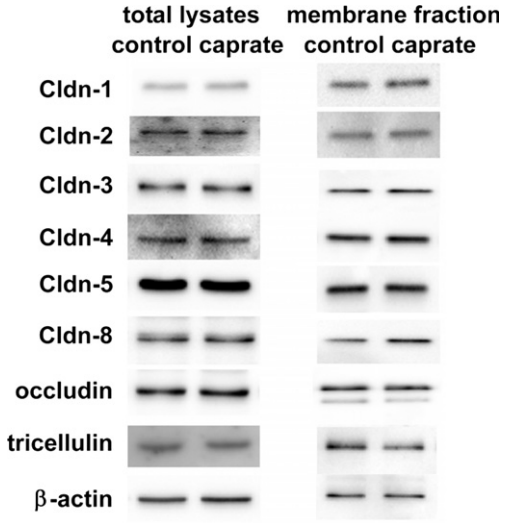

Fig. 5. Effect of caprate on TJ proteins: Western blots. Western blot analysis performed with total lysates and membrane fractions of control and sodium caprate-treated cells (120 min) showed no obvious effects of caprate on TJ protein expressions ($n = 6$). Sensitivity of detection of single proteins varied in both approaches, which was not considered to indicate quantitative differences between the two preparative protocols.

4.3. Modulation of tight junctions for macromolecule passage

Major molecular determinant for paracellular permeability is the TJ, which is primarily composed of tetraspan proteins, occludin [17], the claudin family [15], and tricellulin [18] which are associated with the cytoskeleton via scaffolding proteins, such as ZO-1. Western blot analysis of membrane lysates of control and sodium caprate-treated cells revealed no marked differences in the expression of TJ proteins. In immunostainings, however, a decrease of tricellulin and claudin-5 became apparent, whereas the localization of other TJ proteins including ZO-1 did not markedly change. However, no effect on the actin cytoskeleton after treatment with sodium caprate was observed, and the effects of caprate on intracellular signal transduction remain to be elucidated.

Previously, the effects of caprate have also been reported in the intestinal cell line Caco-2 [50], and MDCK cells. In Caco-2-cells, effects on barrier function were mainly attributed to mechanisms mediated via actin–myosin interactions, which were assumed to result in a retrieval of tight junction proteins from the apicolateral membrane [51,52]. However, this cell line only possesses low endogenous expression of (i) claudin-5, and (ii) tricellulin; the structural correlate for tricellular macromolecule permeability, has not been analyzed. Independently, an effect on claudin-5 by caprate in MDCK cells has been reported [53,54] but an explanation for the

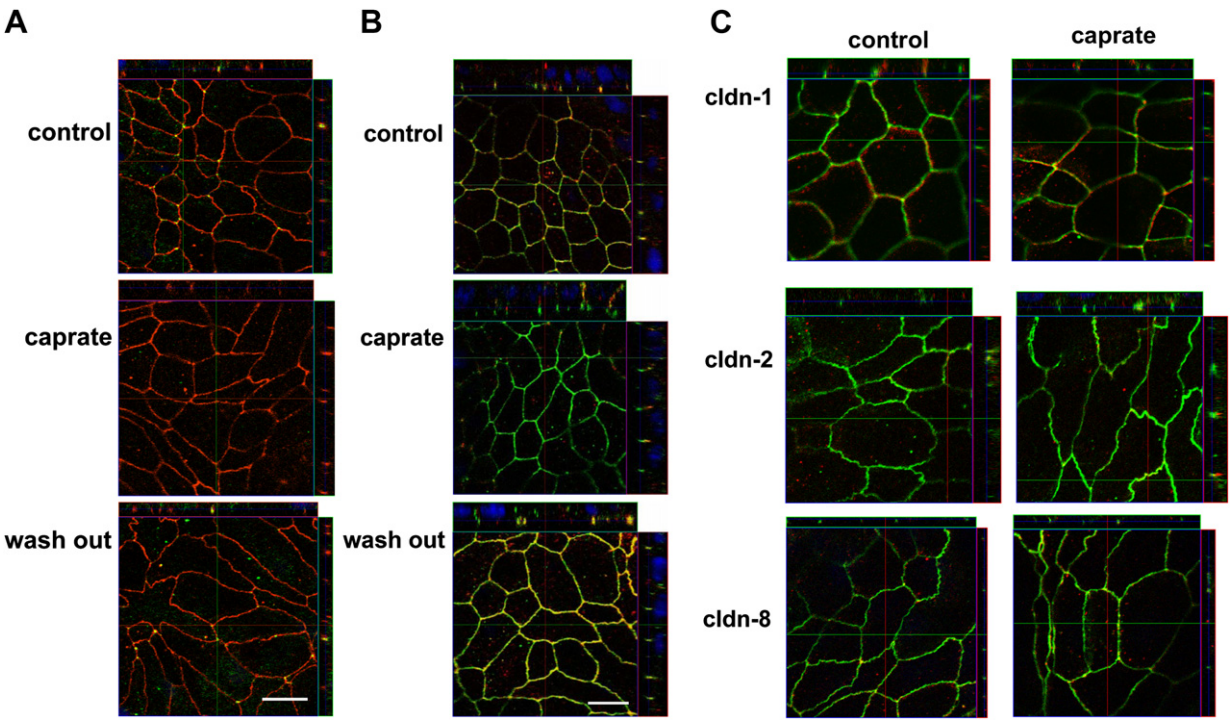

Fig. 6. Confocal laser-scanning immunofluorescence microscopy. Immunofluorescent staining of tight junction proteins. (A) Occludin (red) and tricellulin (green), (B) occludin (green) and claudin-5 (red), and (C) occludin (green) and claudin-1, -2, and -8 (red), respectively. In controls, tricellulin was detected in and was limited to tricellular tight junctions, and claudin-1, -2, -5, and -8 colocalized with occludin also in bicellular tight junctions. Caprate induced a decrease of tricellulin and claudin-5 signals, which was reversible after wash out. (For interpretation of the references to color in this figure legend, the reader is referred to the web version of this article.)

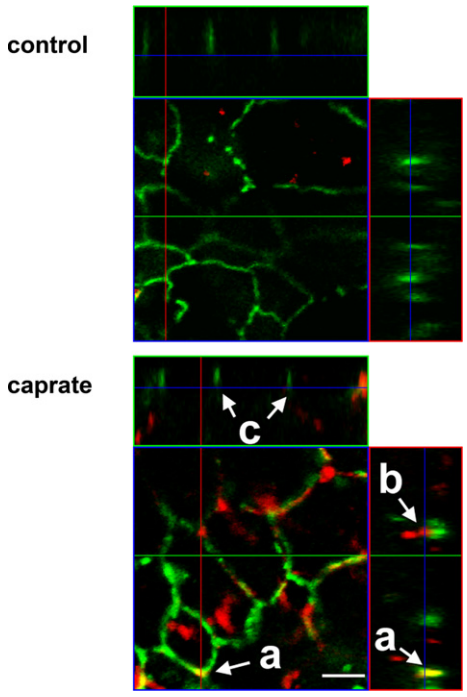

Fig. 7. Visualization of macromolecule translocation site. Apical sulfo-NHS-SS-biotin (606.7 Da) labeling (red) for 2 min prior to fixation and immunofluorescent staining with anti-ZO-1 revealed biotin signals within (a) and below (b) tricellular cell contacts, whereas bicellular tight junctions did not show biotin permeation (c). (For interpretation of the references to color in this figure legend, the reader is referred to the web version of this article.)

altered macromolecule permeability had not been addressed in detail. In our study, we focused on the HT-29/B6 cell line which shows characteristics of colonic epithelia and endogenously expresses claudin-5 and tricellulin, among other major barrier-determining tight junction proteins reported along the longitudinal intestinal axis [20]. Tricellulin has been reported to specifically contribute to the barrier for macromolecules in tTJs [21], which is supported in our study. After treatment with sodium caprate, we detected tricellular passage of sulfo-NHS-SS-biotin (607 Da), a cell membrane-impermeable biotin derivative.

Blocker experiments focusing on actin–myosin interaction and selective inhibition of several single protein kinases did not abolish the caprate effect. Our guess is that intracellular signal transduction may include multiple pathways, so that its final elucidation would be beyond the scope of the present study. However, the simultaneous decrease of tricellulin in tTJs and claudin-5 in bTJs may explain the parallel effects on resistances (indicating reciprocal permeability for small ions) and macromolecule permeability.

Among the mechanisms discussed, caprate could also selectively influence the solubility of membrane microdomains primarily associated with claudin-5 and tricellulin, whereas others could be less affected. Immunochemical analyses detecting protein fractions of different solubility did not reveal further details yet. Our experiments revealed that simultaneous effects can be monitored in bicellular and tricellular cell contacts, with targeted induction of specific macromolecule permeability in tricellular cell contacts.

5. Conclusions

Caprate induces in intestinal epithelial monolayers a fast and reversible TER decrease, which is based on a change in paracellular (i.e. tight junction) resistance, while the transcellular (i.e. cell

membrane) resistance was unaffected. Most importantly, it opens the paracellular pathway for the passage of molecules up to 10 kDa. Since claudin-5, a sealing tight junction protein, is retrieved from bicellular tight junctions, it is most plausible that this effect caused decrease in paracellular resistance and TER, indicating an increased permeability for small ions. Moreover, the enhanced passage of larger molecules appears to take place mainly through the tricellular junction and is triggered by the removal of tricellulin from the tricellular junction. Kinetics and reversibility of the mechanism indicate sodium caprate as a promising candidate for development of intestinal delivery strategies for drugs in the range up to 10 kDa. These results explain and support caprate application as a well tolerated absorption enhancer, and provide insights into the dynamic organization of tight junctions by a compound which is already clinically employed.

Acknowledgments

We thank Detlef Sorgenfrei, In-Fah Lee, and Anja Fromm for their expert technical assistance. This work was supported by grants of the Deutsche Forschungsgemeinschaft (DFG FOR 721/2 and SFB 852) and the Sonnenfeld-Stiftung Berlin.

References

[1] Walsh G. Market development of biopharmaceuticals. In: Engelhard M, Hagen K, Boysen M, editors. Genetic engineering in livestock. New applications and interdisciplinary perspectives. Berlin: Springer; 2009. p. 69–89.
[2] Rosenthal R, Heydt MS, Amasheh M, Stein C, Fromm M, Amasheh S. Analysis of absorption enhancers in epithelial cell models. Ann N Y Acad Sci 2012;1258: 86–92.
[3] Döring F, Walter J, Will J, Föcking M, Boll M, Amasheh S, et al. Delta-aminolevulinic acid transport by intestinal and renal peptide transporters and its physiological and clinical implications. J Clin Invest 1998;101:2761–7.
[4] Amasheh S, Wenzel U, Boll M, Dorn D, Weber W, Clauss W, et al. Transport of charged dipeptides by the intestinal H+/peptide symporter PepT1 expressed in *Xenopus laevis* oocytes. J Membr Biol 1997;155:247–56.
[5] Döring F, Will J, Amasheh S, Clauss W, Ahlbrecht H, Daniel H. Minimal molecular determinants of substrates for recognition by the intestinal peptide transporter. J Biol Chem 1998;273:23211–8.
[6] Rosenthal R, Günzel D, Finger C, Krug SM, Richter JF, Schulzke JD, et al. Chitosan opens the epithelial barrier via rapid transcellular and paracellular effects. Biomaterials 2012;33:2791–800.
[7] Lindmark T, Söderholm JD, Olaison G, Alván G, Ocklind G, Artursson P. Mechanism of absorption enhancement in humans after rectal administration of ampicillin in suppositories containing sodium caprate. Pharm Res 1997;14: 930–5.
[8] Johnson LG, Vanhook MK, Coyne CB, Haykal-Coates N, Gavett SH. Safety and efficiency of modulating paracellular permeability to enhance airway epithelial gene transfer in vivo. Hum Gene Ther 2003;14:729–47.
[9] Morishita M, Morishita I, Takayama K, Machida Y, Nagai T. Site-dependent effect of aprotinin, sodium caprate, Na2EDTA and sodium glycocholate on intestinal absorption of insulin. Biol Pharm Bull 1993;16:68–72.
[10] Lindmark T, Schipper N, Lazorová L, de Boer AG, Artursson P. Absorption enhancement in intestinal epithelial caco-2 monolayers by sodium caprate: assessment of molecular weight dependence and demonstration of transport routes. J Drug Target 1998;5:215–23.
[11] Jensen RG. Fatty acids in milk and dairy products. In: Chow CK, editor. Fatty acids in foods and their implications. NY: Marcel Dekker; 2000. p. 109–23.
[12] Lower ES. Capric acid-uses and properties part 1. Manuf Chem 1984;55:61–3.
[13] US Food and Drug Administration. Salts of fatty acids. In: Food additives permitted for direct addition to food for human consumption, CFR 21, part 3; 2008. section 172.860.
[14] Günzel D, Fromm M. Claudins and other tight junction proteins. Compr Physiol 2012;2:1819–52.
[15] Furuse M, Fujita K, Hiiragi T, Fujimoto K, Tsukita S. Claudin-1 and -2: novel integral membrane proteins localizing at tight junctions with no sequence similarity to occludin. J Cell Biol 1998;141:1539–50.
[16] Raleigh DR, Marchiando AM, Zhang Y, Shen L, Sasaki H, Wang Y, et al. Tight junction-associated MARVEL proteins marveld3 tricellulin and occludin have distinct but overlapping functions. Mol Biol Cell 2010;7:1200–13.
[17] Furuse M, Hirase T, Itoh M, Nagafuchi A, Yonemura S, Tsukita S. Occludin: a novel integral membrane protein localizing at tight junctions. J Cell Biol 1993;123:1777–88.
[18] Ikenouchi J, Furuse M, Furuse K, Sasaki H, Tsukita S. Tricellulin constitutes a novel barrier at tricellular contacts of epithelial cells. J Cell Biol 2005;171: 939–45.
[19] Steed E, Rodrigues NT, Balda MS, Matter K. Identification of marveld3 as a tight junction-associated transmembrane protein of the occludin family. BMC Cell Biol 2009;10:95.
[20] Markov AG, Veshnyakova A, Fromm M, Amasheh M, Amasheh S. Segmental expression of claudin proteins correlates with tight junction barrier properties in rat intestine. J Comp Physiol B 2010;180:591–8.
[21] Tebbe B, Mankertz J, Schwarz C, Amasheh S, Fromm M, Assaf C, et al. Tight junction proteins: a novel class of integral membrane proteins. Expression in human epidermis and in HaCaT keratinocytes. Arch Dermatol Res 2002;294: 14–8.
[22] Markov AG, Kruglova NM, Fomina YA, Fromm M, Amasheh S. Altered expression of tight junction proteins in mammary epithelium after discontinued suckling in mice. Pflugers Arch Eur J Physiol 2012;463:391–8.
[23] Markov AG, Voronkova MA, Volgin GN, Yablonsky PK, Fromm M, Amasheh S. Tight junction proteins contribute to barrier properties in human pleura. Respir Physiol Neurobiol 2011;175:331–5.
[24] Amasheh S, Fromm M, Günzel D. Claudins of intestine and nephron – a correlation of molecular tight junction structure and barrier function. Acta Physiol (Oxf) 2011;201:133–40.
[25] Furuse M, Hata M, Furuse K, Yoshida Y, Haratake A, Sugitani Y, et al. Claudin-based tight junctions are crucial for the mammalian epidermal barrier: a lesson from claudin-1-deficient mice. J Cell Biol 2002;156: 1099–111.
[26] Milatz S, Krug SM, Rosenthal R, Günzel D, Müller D, Schulzke JD, et al. Claudin-3 acts as a sealing component of the tight junction for ions of either charge and uncharged solutes. Biochim Biophys Acta 2010;1798:2048–57.
[27] Amasheh S, Schmidt T, Mahn M, Florian P, Mankertz J, Tavalali S, et al. Contribution of claudin-5 to barrier properties in tight junctions of epithelial cells. Cell Tissue Res 2005;321:89–96.
[28] Amasheh S, Meiri N, Gitter AH, Schöneberg T, Mankertz J, Schulzke JD, et al. Claudin-2 expression induces cation-selective channels in tight junctions of epithelial cells. J Cell Sci 2002;115:4969–76.
[29] Günzel D, Stuiver M, Kausalya PJ, Haisch L, Rosenthal R, Krug SM, et al. Claudin-10 exists in six alternatively spliced isoforms which exhibit distinct localization and function. J Cell Sci 2009;122:1507–17.
[30] Tamura A, Hayashi H, Imasato M, Yamazaki Y, Hagiwara A, Wada M, et al. Loss of claudin-15, but not claudin-2, causes Na^+ deficiency and glucose malabsorption in mouse small intestine. Gastroenterology 2010;140:913–23.
[31] Krug SM, Günzel D, Conrad MP, Rosenthal R, Fromm A, Amasheh S, et al. Claudin-17 forms tight junction channels with distinct anion selectivity. Cell Mol Life Sci 2012;69(69):2765–78.
[32] Takahashi A, Saito Y, Kondoh M, Matsushita K, Krug SM, Suzuki H, et al. Creation and biochemical analysis of a broad-specific claudin binder. Biomaterials 2012;33:3464–74.
[33] Krug SM, Amasheh S, Richter JF, Milatz S, Günzel D, Westphal JK, et al. Tricellulin forms a barrier to macromolecules in tricellular tight junctions without affecting ion permeability. Mol Biol Cell 2009;20: 3713–24.
[34] Staehelin LA. Further observations of the fine structure of freezecleaved tight junctions. J Cell Sci 1973;13:763–86.
[35] Wade JB, Karnovsky MJ. The structure of the zonula occludens. A single fibril model based on freeze-fracture. J Cell Biol 1974;60:168–80.
[36] Walker DC, MacKenzie A, Hosford S. The structure of the tricellular region of endothelial tight junctions of pulmonary capillaries analyzed by freeze fracture. Microvasc Res 1994;48:259–81.
[37] Staehelin LA, Mukherjee TM, Williams AW. Freeze-etch appearance of tight junctions in the epithelium of small and large intestine of mice. Protoplasma 1969;67:165–84.
[38] Walker DC, MacKenzie A, Hulbert WC, Hogg JC. A re-assessment of the tricellular region of epithelial cell tight junctions in trachea of guinea pig. Acta Anat 1985;122:35–8.
[39] Maher S, Leonard TW, Jacobsen J, Brayden DJ. Safety and efficacy of sodium caprate in promoting oral drug absorption: from in vitro to the clinic. Adv Drug Deliv Rev 2009;61:1427–49.
[40] Anderberg EK, Lindmark T, Artursson P. Sodium caprate elicits dilatations in human intestinal tight junctions and enhances drug absorption by the paracellular route. Pharm Res 1993;10:857–64.
[41] Kimura Y, Hosoda Y, Yamaguchi M, Nagano H, Shima M, Adachi S, et al. Effects of medium-chain fatty acids on intracellular calcium levels and the cytoskeleton in human intestinal (caco-2) cell monolayers. Biosci Biotechnol Biochem 2001;65:743–51.
[42] Feighery LM, Cochrane SW, Quinn T, Baird AW, O'Toole D, Owens SE, et al. Myosin light chain kinase inhibition: correction of increased intestinal epithelial permeability in vitro. Pharm Res 2008;25:1377–86.
[43] Kreusel KM, Fromm M, Schulzke JD, Hegel U. Cl^- secretion in epithelial monolayers of mucus-forming human colon cells (HT-29/B6). Am J Physiol 1991;261:C574–82.
[44] Madara JL, Stafford J. Interferon-gamma directly affects barrier function of cultured intestinal epithelial monolayers. J Clin Invest 1989;83:724–7.
[45] Krug SM, Fromm M, Günzel D. Two-path impedance spectroscopy for measuring paracellular and transcellular epithelial resistance. Biophys J 2009; 97:2202–11.

[46] Amasheh M, Fromm A, Krug SM, Amasheh S, Andres S, Zeitz M, et al. TNFalpha-induced and berberine-antagonized tight junction barrier impairment via tyrosine kinase, Akt and NFkappaB signaling. J Cell Sci 2012;123:4145–55.
[47] Amasheh S, Milatz S, Krug SM, Bergs M, Amasheh M, Schulzke JD, et al. Na^+ absorption defends from paracellular back-leakage by claudin-8 upregulation. Biochem Biophys Res Commun 2009;378:45–50.
[48] Bjarnason I. Intestinal permeability. Gut 1994;35:S18–22.
[49] Wolfe MM, Lichtenstein DR, Singh G. Gastrointestinal toxicity of nonsteroidal antiinflammatory drugs. N Engl J Med 1999;340:1888–99.
[50] Turner JR. 'Putting the squeeze' on the tight junction: understanding cytoskeletal regulation. Semin Cell Dev Biol 2000;11:301–8.
[51] Sakai M, Imai T, Ohtake H, Azuma H, Otagiri M. Effects of absorption enhancers on cytoskeletal actin filaments in caco-2 cell monolayers. Life Sci 1998;63:45–54.
[52] Lindmark T, Kimura Y, Artursson P. Absorption enhancement through intracellular regulation of tight junction permeability by medium chain fatty acids in caco-2 cells. J Pharmacol Exp Ther 1998;284:362–9.
[53] Sugibayashi K, Onuki Y, Takayama K. Displacement of tight junction proteins from detergent-resistant membrane domains by treatment with sodium caprate. Eur J Pharm Sci 2009;36:246–53.
[54] Del Vecchio G, Tscheik C, Tenz K, Helms HC, Winkler L, Blasig R, et al. Sodium caprate transiently opens claudin-5-containing barriers at tight junctions of epithelial and endothelial cells. Mol Pharm 2012;9:2523–33.